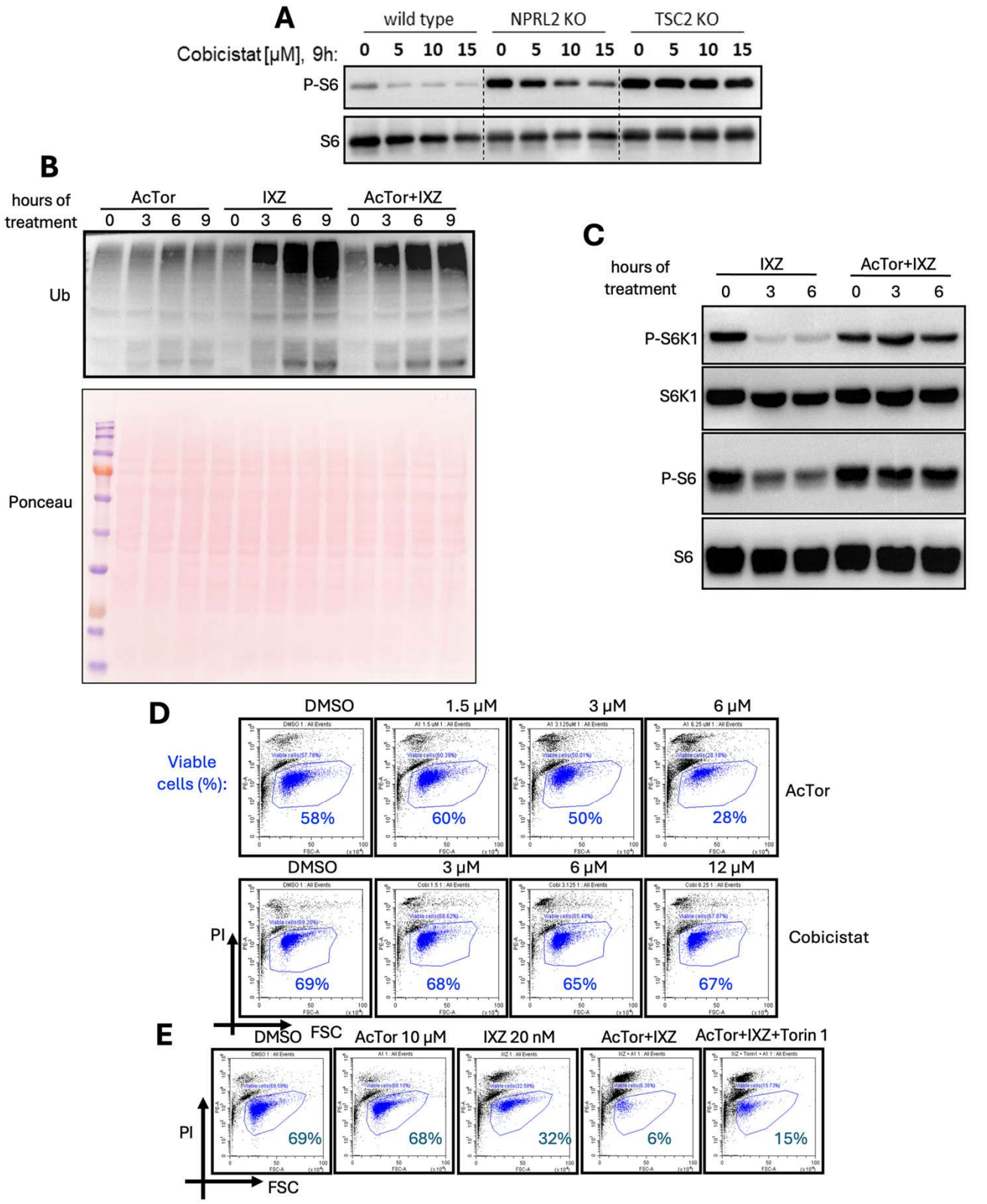

Figure S1: AcTor synergizes with IXZ without affecting proteasome inhibition activity: (A) RPMI 8226 cells were treated with the indicated concentrations of cobicistat. mTORC1activity was assessed by immunoblotting for P-S6. We used control cells and two mutants. NPRL2 KO that activates mTORC1 through the amino acid sensing pathway, and TSC2 KO. Only TSC2 KO cells maintained mTORC1 activity in the presence of cobicistat. **(B)** RPMI 8226 cells were treated with IXZ (20 nM), AcTor (10 μM) or both. Ubiquitination was assessed by immunoblotting. **(C)** RPMI 8226 cells were treated with IXZ (20 nM) in the presence and absence of AcTor (10 μM) for the indicated times. mTORC1activity was assessed by immunoblotting. **(D)** RPMI 8226 cells were treated for 72 h with AcTor or Cobicistat. Shown is one of two similar experiments. **(E)** Viability of RPMI 8226 cells following 24 h treatment with the indicated drugs was assessed by flow cytometry using propidium iodide as vital stain. In blue are the live cells. Shown is one of two similar experiments.

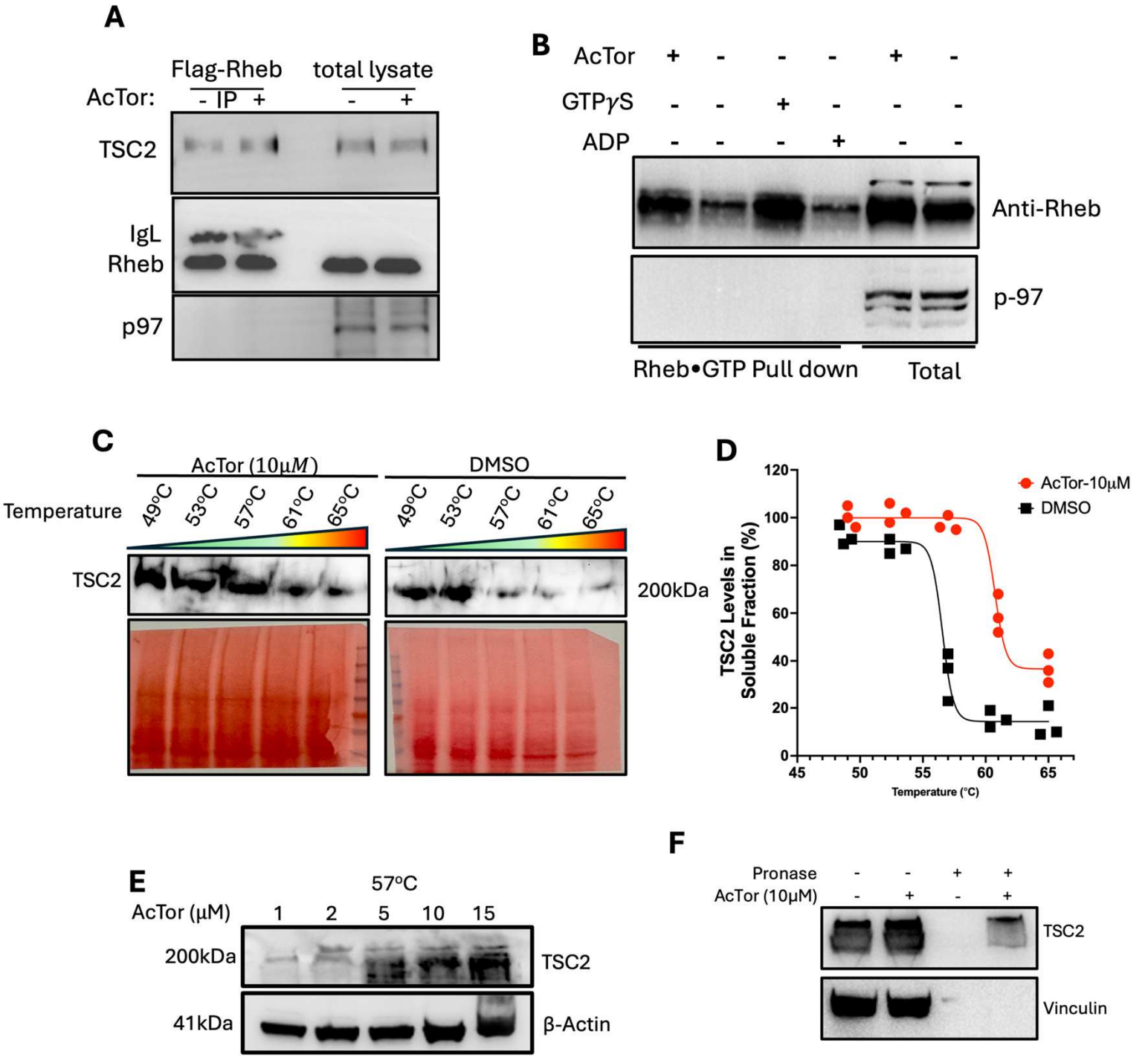

Figure S2: Indirect evidence of AcTor binding to TSC2: Thermostability assays were performed according to (PMID: 35391936). **(A)** 293T cells were transfected with FLAG-Rheb. Cells were treated with AcTor (10 μM) for 24 h and lysates were prepared in 1% NP-40 containing lysing buffer. Anti-FLAG immunoprecipitates were analyzed by immunoblotting for TSC2. **(B)** MV4-11 were treated with AcTor (10 μM) for 24 h, lysed and Rheb•GTP was immunoprecipitated with anti-Rheb•GTP monoclonal antibody, followed by immunoblotting with polyclonal anti-Rhed. Spiking the lysates with GTPγS or GDP were used as a positive and negative control, respectively. Shown is one of two similar experiments. **(C)** MV4-11 cells were treated with AcTor (10 μM) for 24 h and heated at the indicated temperatures in PBS supplemented with protease inhibitor cocktail. Cell lysates were subjected to harsh centrifugation, and the soluble fraction was analyzed by immunoblotting. **(D)** Shown are the levels of soluble TSC2 vs total levels of three independent experiments, quantified by densitometry and normalized to 49°C reading. **(E)** MV4-11 cells were incubated for 24 h with AcTor and analyzed as in C for soluble TSC2. Maximal level of soluble TSC2 was observed at approximately 10-15 μM (F) MV4-11 cell lysates were incubated with AcTor or DMSO. Lysates were prepared, protein content quantified and pronase was added at 300:1 ratio. Immunoblot for TSC2 demonstrate protection by AcTor relative to DMSO controls. Shown is one of two repetitions.

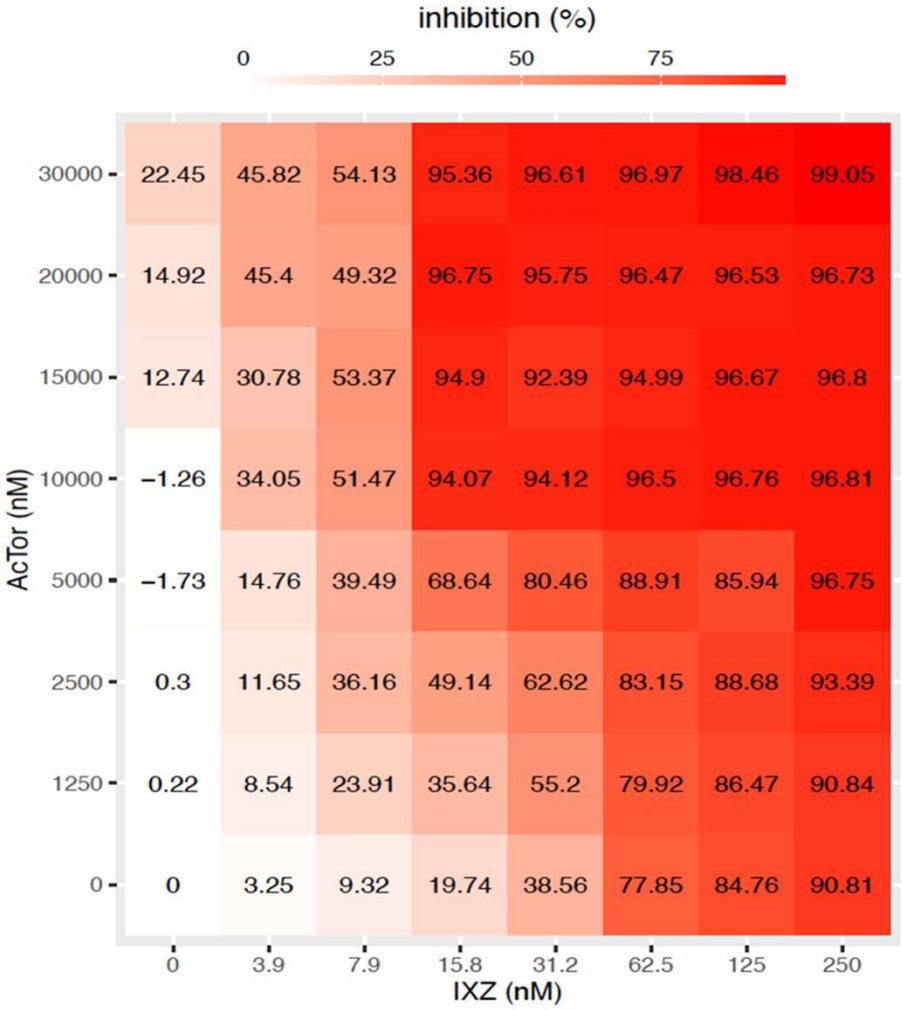

Figure S3: Synergism of AcTor and IXZ. MV4-11 cells were treated with 7 different concentrations of AcTor and 7 different concentrations of IXZ at all possible combinations. After 24 hours of treatment, cell viability was quantified using the CellTiter-Glo assay. Drug interaction effects were analyzed using the SynergyFinder platform employing the Bliss independence model to calculate synergy scores.

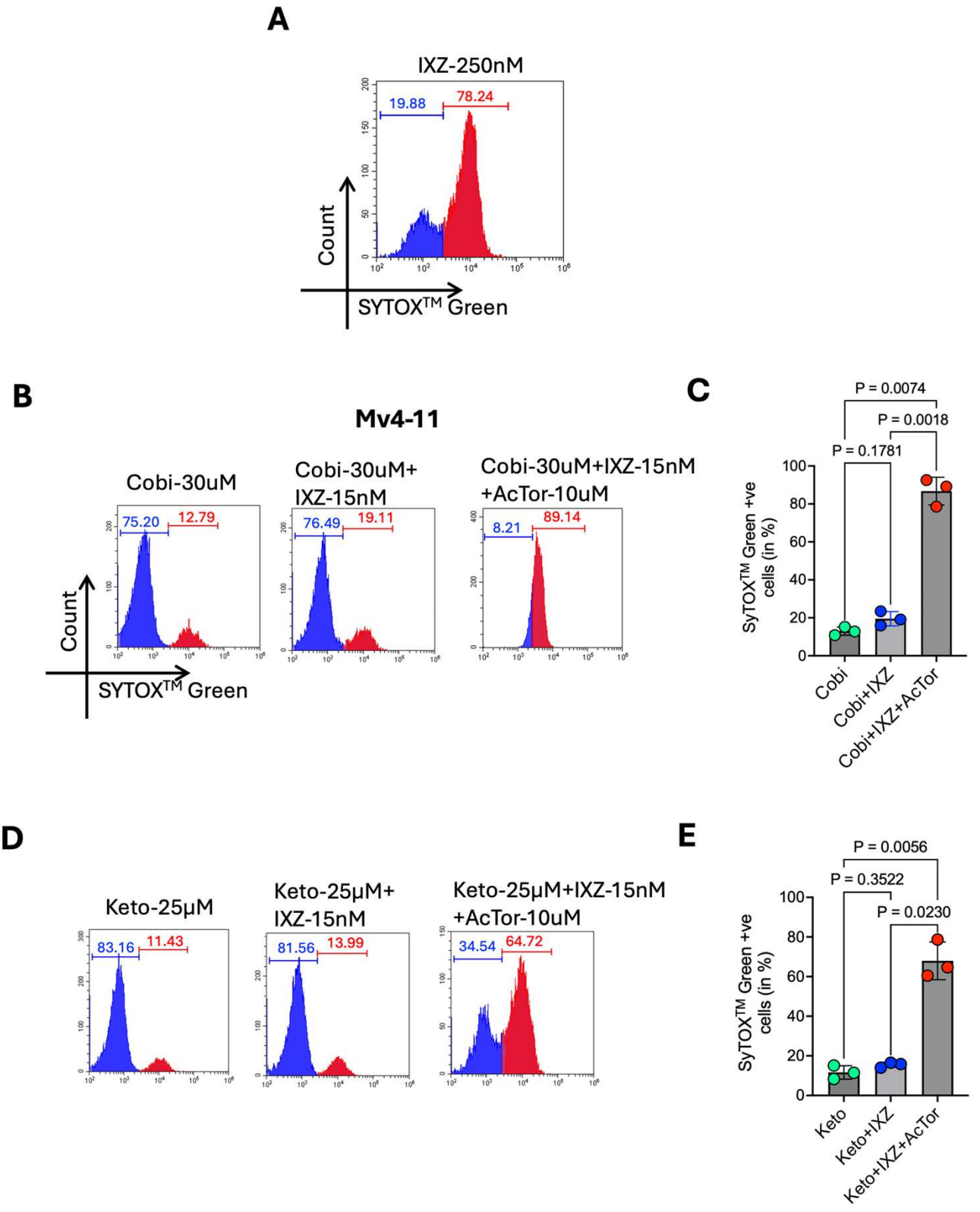

Figure S4: Synergism between AcTor and IXZ is not related to CYP inhibition: (A) MV4-11 cells were incubated for 24 h with IXZ alone. Viability was determined by flow cytometry using SyTox Green as a vital dye. **(B)** MV4-11 cells were treated with Cobicistat (30 μM) with and without IXZ (15 nM) for 24 h. AcTor was added to the combination to demonstrate its necessity for synergism. **(C)** Quantification of three independent experiments. **(D)** MV4-11 cells were treated with Ketoconazole (25 μM) with and without IXZ (15 nM) for 24 h. AcTor was added to the combination to demonstrate the CYP independent synergy. **(E)** Quantification of three independent experiments. Data are presented as mean ± SD from n=3 independent biological replicates. Statistical significance was determined using Brown-Frosythe and Welch one-way ANOVA followed by Dunnett's T3 multiple comparisons test. Exact P values are indicated in the graphs.

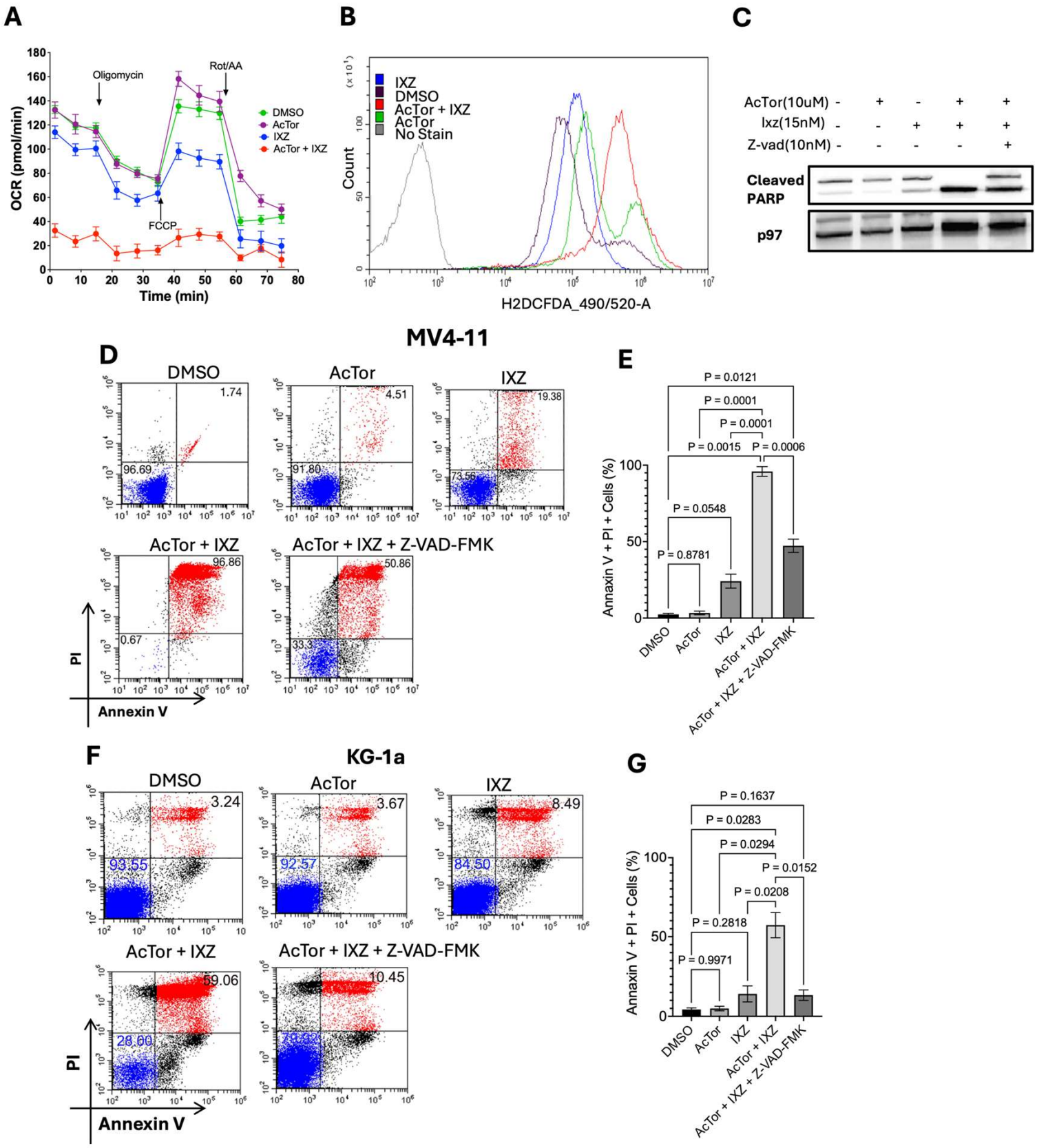

Figure S5: AcTor/IXZ induces intrinsic apoptosis: (A) MV4-11 cells were incubated for 24 h with DMSO, IXZ, AcTor and AcTor+IXZ. ROS production was assessed by H2DCFDA staining. Shown is a representative result of three independent experiments. **(B)** MV4-11 cells were treated the indicated drugs for for 24 h. Cells were lysed and analyzed by immunoblotting for PARP1. Shown is a representative Western blot of three independent experiments. **(C)** MV4-11 cells or KG-1a **(D)** were treated as in A for 24 h and apoptosis was assessed by propidium iodide/Annexin V staining. Z-VAD-fmk was added to assess apoptosis. Data are presented as mean ± SD from n=3 independent biological replicates. Statistical significance was determined using Brown-Frosythe and Welch one-way ANOVA followed by Dunnett's T3 multiple comparisons test. Exact P values are indicated in the graphs.

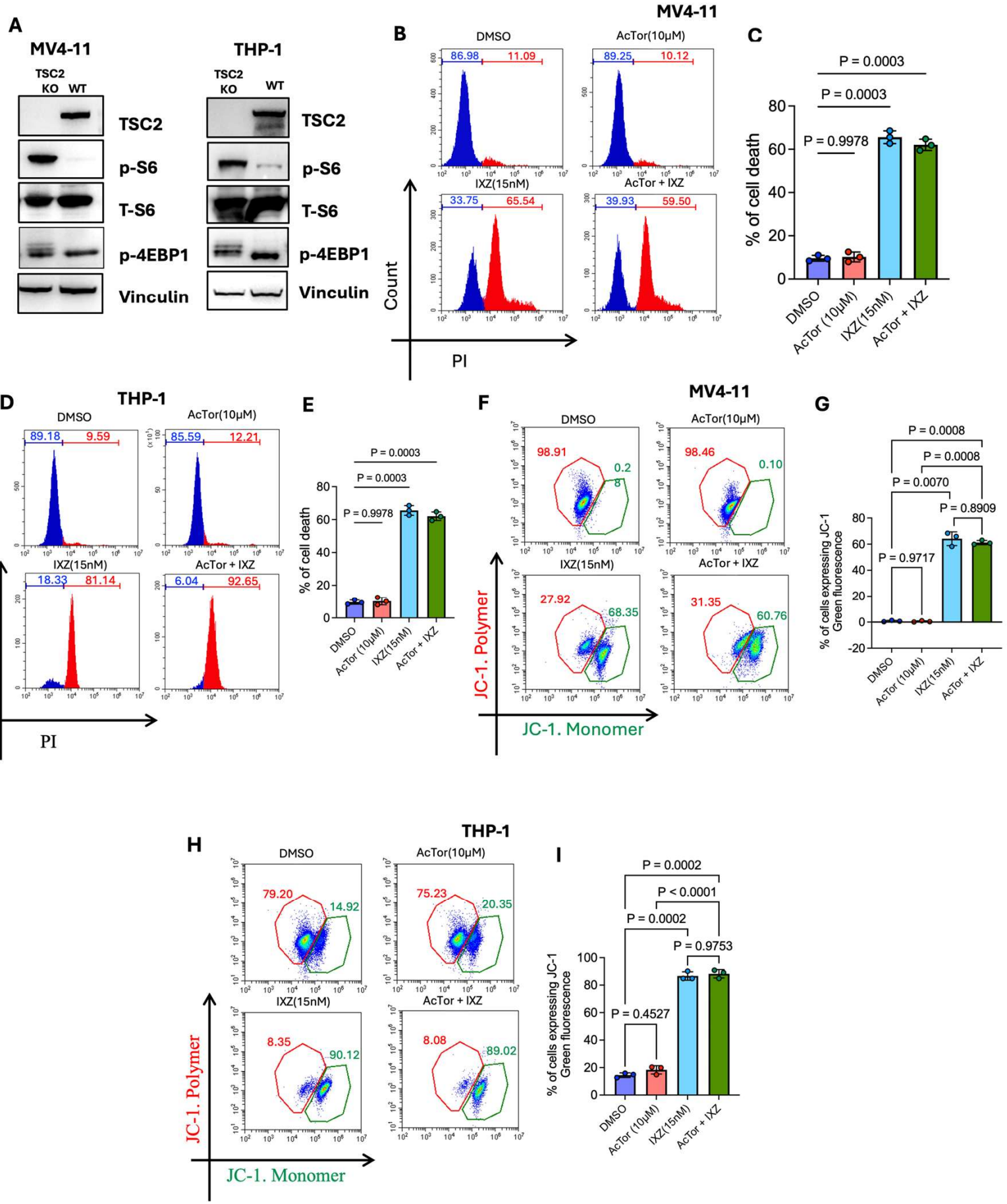
A
MV4-11
TSC2 KO
WT
TSC2
p-S6
T-S6
p-4EBP1
Vinculin
THP-1
TSC2 KO
WT
TSC2
p-S6
T-S6
p-4EBP1
Vinculin
B
MV4-11
DMSO
AcTor(10μM)
86.98
11.09
89.25
10.12
IXZ(15nM)
AcTor + IXZ
33.75
65.54
39.93
59.50
Count
PI
C
P = 0.0003
P = 0.0003
P = 0.9978
% of cell death
DMSO
AcTor (10μM)
IXZ(15nM)
AcTor + IXZ
D
THP-1
DMSO
AcTor(10μM)
89.18
9.59
85.59
12.21
IXZ(15nM)
AcTor + IXZ
18.33
81.14
6.04
92.65
Count
PI
E
P = 0.0003
P = 0.0003
P = 0.9978
% of cell death
DMSO
AcTor (10μM)
IXZ(15nM)
AcTor + IXZ
F
MV4-11
DMSO
AcTor(10μM)
98.91
0.2
98.46
0.10
IXZ(15nM)
AcTor + IXZ
27.92
68.35
31.35
60.76
JC-1. Polymer
JC-1. Monomer
G
P = 0.0008
P = 0.0008
P = 0.0070
P = 0.8909
P = 0.9717
% of cells expressing JC-1 Green fluorescence
DMSO
AcTor (10μM)
IXZ(15nM)
AcTor + IXZ
H
THP-1
DMSO
AcTor(10μM)
79.20
14.92
75.23
20.35
IXZ(15nM)
AcTor + IXZ
8.35
90.12
8.08
89.02
JC-1. Polymer
JC-1. Monomer
I
P = 0.0002
P < 0.0001
P = 0.0002
P = 0.9753
P = 0.4527
% of cells expressing JC-1 Green fluorescence
DMSO
AcTor (10μM)
IXZ(15nM)
AcTor + IXZ

Figure S6: Genetic inhibition of TSC2 phenocopies AcTor and renders cells insensitive to AcTor-mediated potentiation. MV4-11 and THP-1 cells were infected with lentiviruses encoding shTSC2. After selection cells were treated for 24 h with DMSO, AcTor, IXZ or the combination. **(A)** Immunoblot analysis of MV4-11 and THP-1 cells confirms reduced TSC2 expression and mTORC1 activation. **(B-E)** Viability analyses of the two shTSC2 cells displayed elevated sensitivity to IXZ alone and the addition of AcTor did not further increase cytotoxicity. **(F-I)** Mitochondrial membrane potential was assessed by JC-1 staining. In both shTSC2 cells IXZ alone induced equivalent mitochondrial collapse, and AcTor did not further enhance depolarization. Data are presented as mean ± SD from n=3 independent biological replicates performed at the same day. Statistical significance was determined using Brown-Frosythe and Welch one-way ANOVA followed by Dunnett's T3 multiple comparisons test. Calculated *P* values are indicated in the graphs.

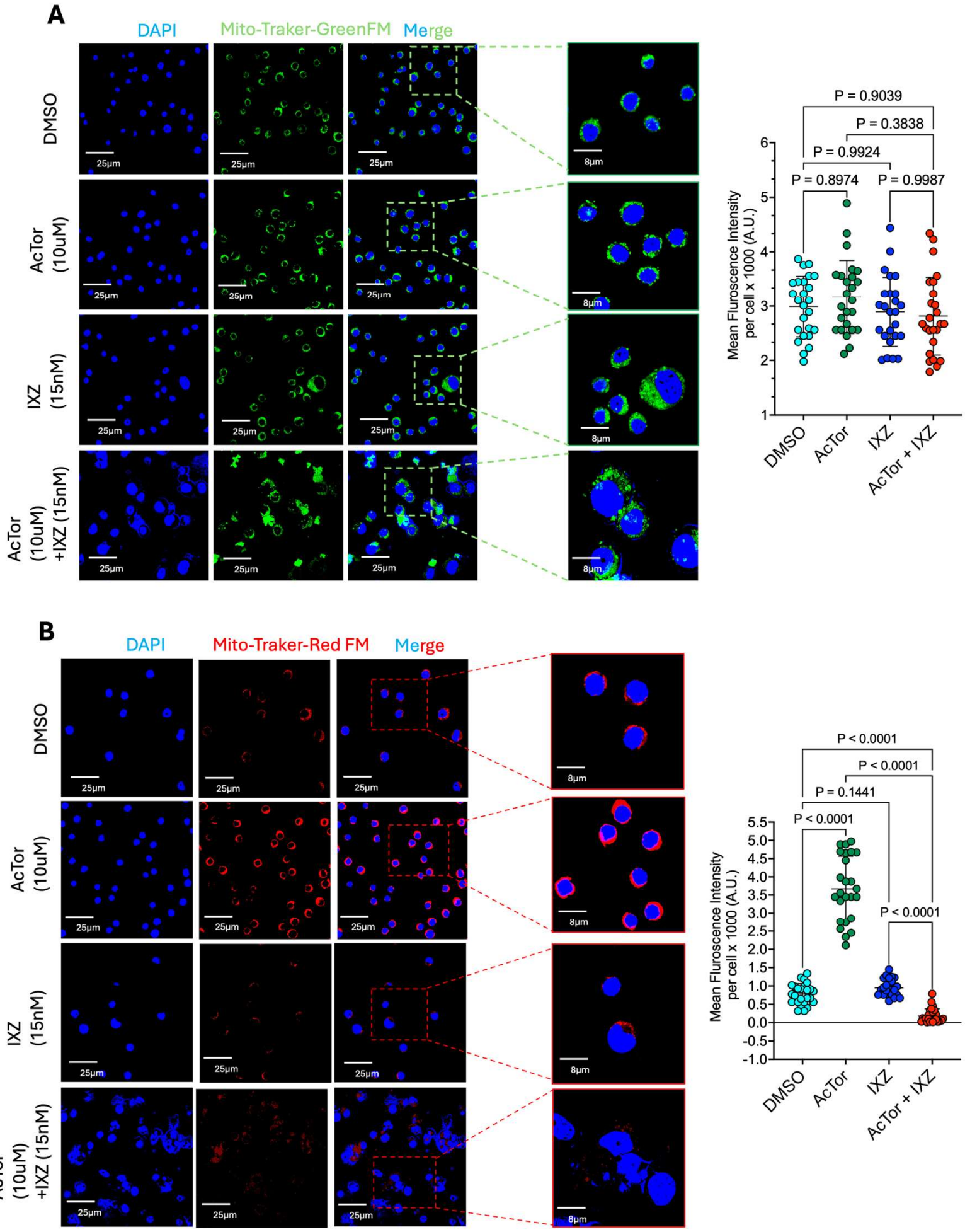
A
DAPI
Mito-Traker-GreenFM
Merge
DMSO
AcTor (10uM)
IXZ (15nM)
AcTor (10uM) +IXZ (15nM)
25μm
8μm
Mean Fluroscence Intensity per cell x 1000 (A.U.)
P = 0.9039
P = 0.3838
P = 0.9924
P = 0.8974
P = 0.9987
DMSO
AcTor
IXZ
AcTor + IXZ
B
DAPI
Mito-Traker-Red FM
Merge
DMSO
AcTor (10uM)
IXZ (15nM)
AcTor (10uM) +IXZ (15nM)
25μm
8μm
Mean Fluroscence Intensity per cell x 1000 (A.U.)
P < 0.0001
P < 0.0001
P = 0.1441
P < 0.0001
P < 0.0001
DMSO
AcTor
IXZ
AcTor + IXZ

Figure S7: AcTor/IXZ treatment reduces mitochondria activity without affecting mitochondria content: (A) MV4-11 cells were incubated for 24 h with DMSO, IXZ, AcTor and AcTor+IXZ for 24h. Cells were stained with MitoTracker Green, which is indicative to mitochondrial content. Shown is the quantification of 25 cells for each treatment. **(B)** MV4-11 cells were incubated for 24 h with DMSO, IXZ, AcTor and AcTor+IXZ for 24 h. Cells were stained with MitoTracker Red, which is sensitive to mitochondrial membrane potential. Shown is the quantification of 20 cells for each treatment. Data are presented as mean ± SD from 20 cells taken from random images. Statistical significance was determined using Brown-Frosythe and Welch one-way ANOVA followed by Dunnett's T3 multiple comparisons test. Calculated *P* values are indicated.

A

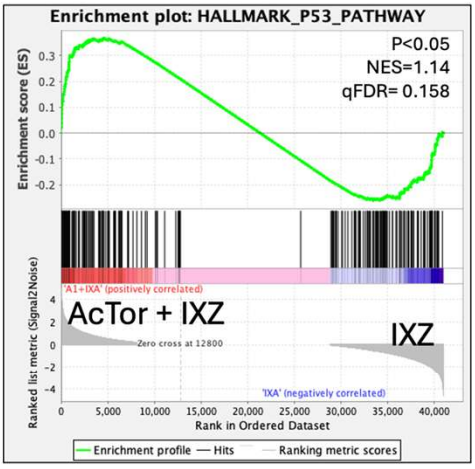

B

AcTor Vs DMSO (upregulation)

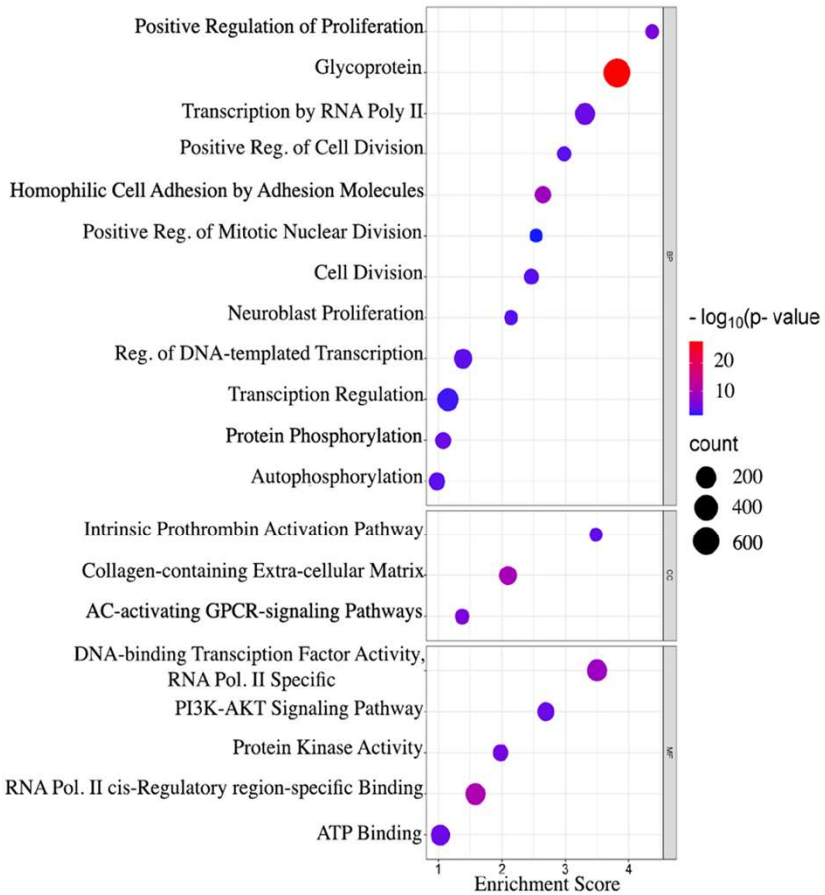

AcTor+IXZ Vs IXZ (upregulation)

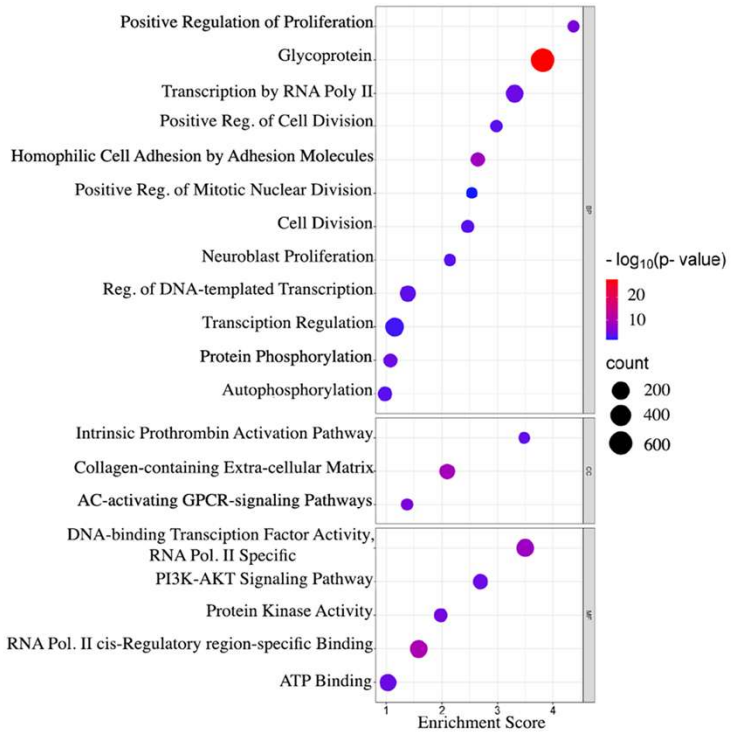

C

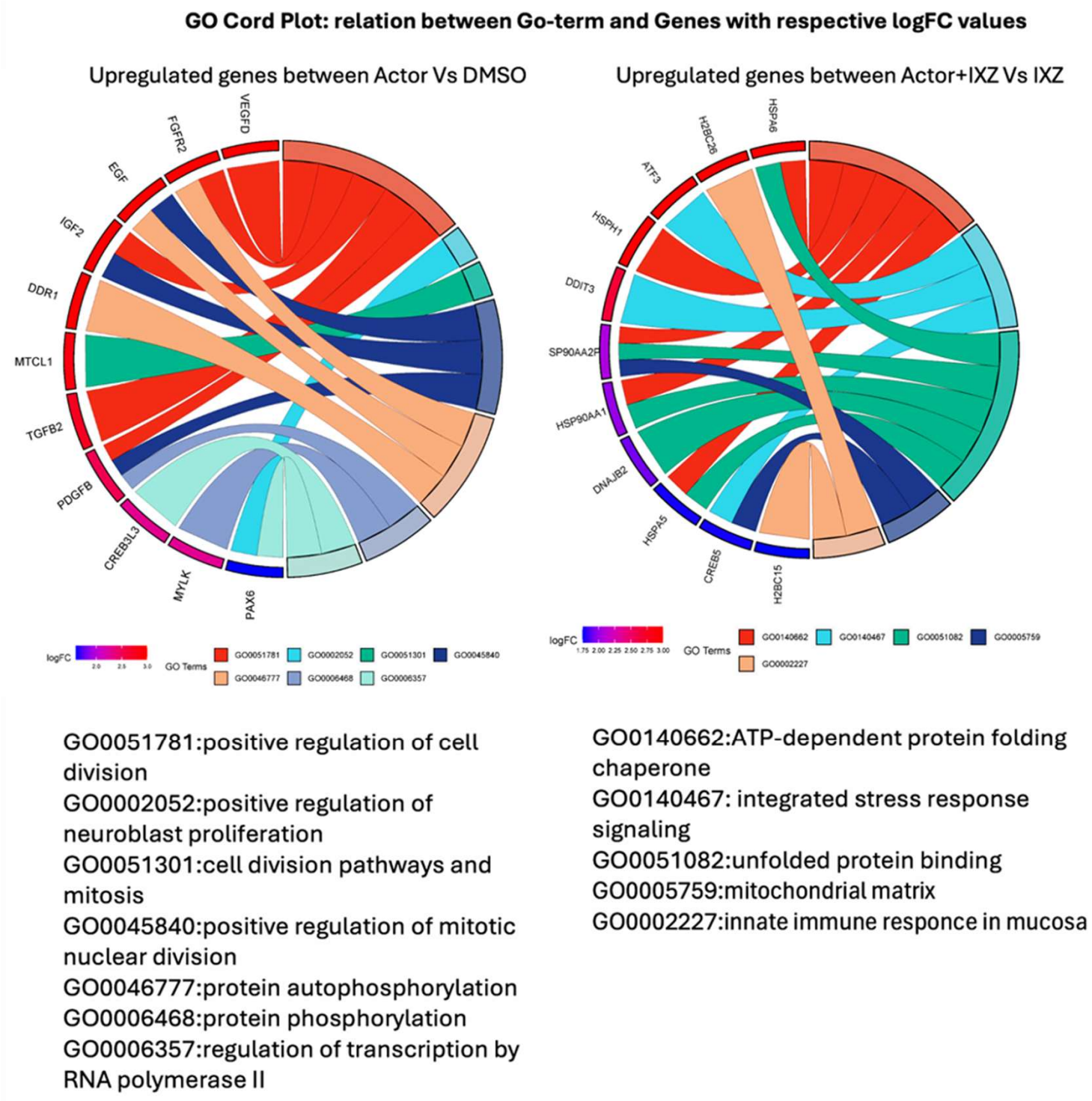

GO0051781:positive regulation of cell division
GO0002052:positive regulation of neuroblast proliferation
GO0051301:cell division pathways and mitosis
GO0045840:positive regulation of mitotic nuclear division
GO0046777:protein autophosphorylation
GO0006468:protein phosphorylation
GO0006357:regulation of transcription by RNA polymerase II

GO0140662:ATP-dependent protein folding chaperone
GO0140467: integrated stress response signaling
GO0051082:unfolded protein binding
GO0005759:mitochondrial matrix
GO0002227:innate immune responce in mucosa

Figure S8: AcTor/IXZ treatment induces a stress response: (A) RNAseq analysis of MV4-11 indicate an enhanced p53 expression signature. **(B)** Bubble plots of the gene ontology analysis of the upregulated genes of AcTor vs DMSO and AcTor/IXZ vs IXZ. A pro-oncogenic pathway was replaced by a stress-related pathway. **(C)** Chord diagram showing the core genes of significant pathways of AcTor vs DMSO and AcTor/IXZ vs IXZ. AcTor alone underscores tyrosine kinase signaling genes, while AcTor/IXZ induces stress related genes.

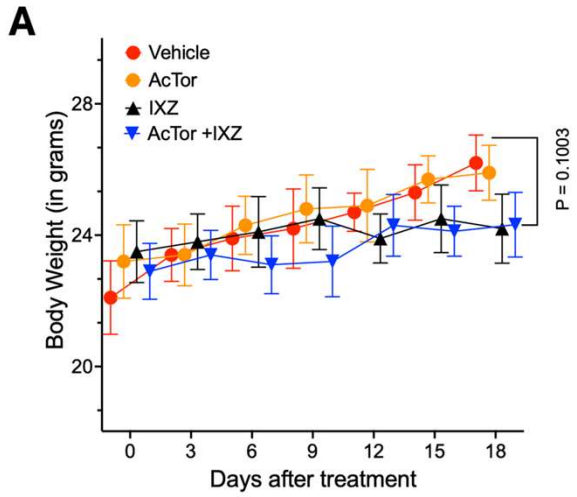

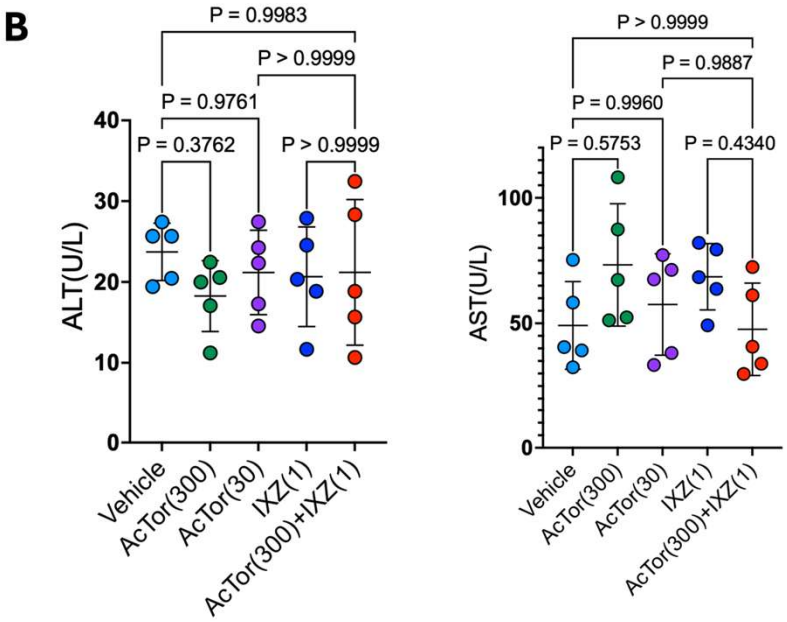

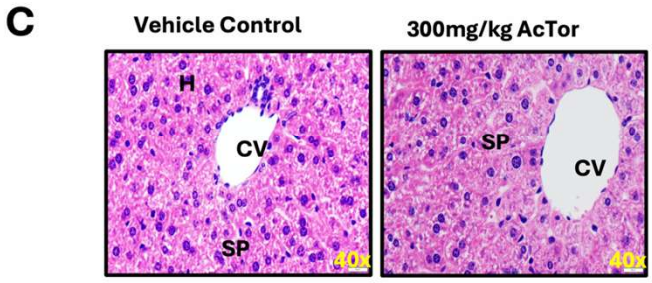

SP : sinusoidal space
CV : Central Vein
H. : Hepatocyte

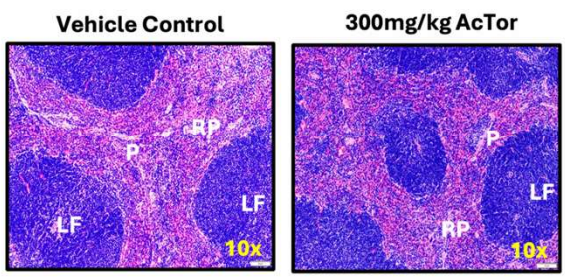

P : Peri Arteriolar Lymphocyte Sheath
RP: Red Pulp
LF: Lymphoid Follicle

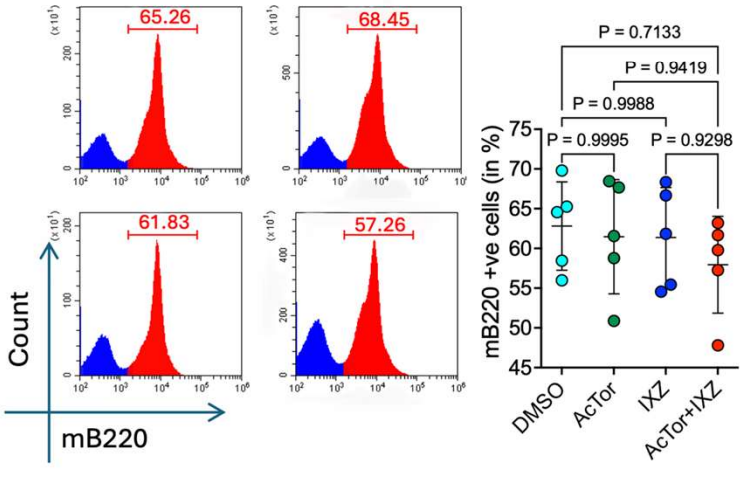

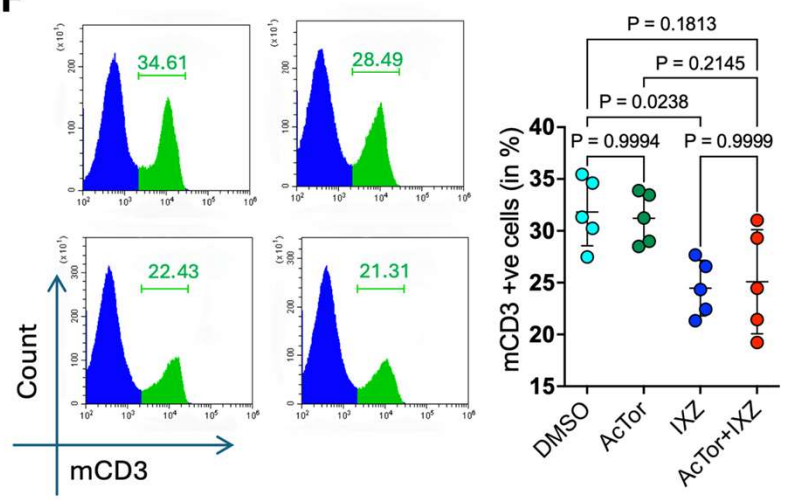

G

Hematology Parameters Measured	Vehicle	AcTor	IXZ	AcTor+IXZ
WBC(10^3/ul)	8.1±2.604	8.99±3.418	7.633±3.061	6.783±1.921
LYM (%)	83.033±2.843	82.65±1.114	85.31±2.680	77.816±2.491
MONO(%)	5.133±0.882	4.016±0.69	4.25±1.029	4.5±0.547
GRAN(%)	11.833±2.33	13.333±0.99	10.43±1.701	15.683±2.095
HCT(%)	44.033±3.091	42.65±1.623	38.93±8.25	45.21±1.811
MCV(femtoliters)	49.95±0.831	47.366±2.99	48.46±2.443	45.9±0.684
RDW(%)	19.716±0.99	18.233±0.45	18.86±0.637	18.76±0.975
HGB(g/dl)	13.65±0.954	13.6±0.377	12.45±2.558	14.51±0.435
MCHC(g/dl)	31.016±0.184	32.016±0.67	32.1±0.565	32.083±0.71
MCH(pg)	15.48±0.21	15.166±0.32	15.55±0.575	14.716±0.172
RBC(10^6/ul)	8.815±0.711	9±0.216	8.03±1.768	9.85±0.341
PLT(10^3/ul)	490.3±77.74	541.16±110.05	536.5±205.73	567±120.40
MPV(femtoliters)	6.183±0.453	6±0.644	6.36±0.496	5.9±0.236

H

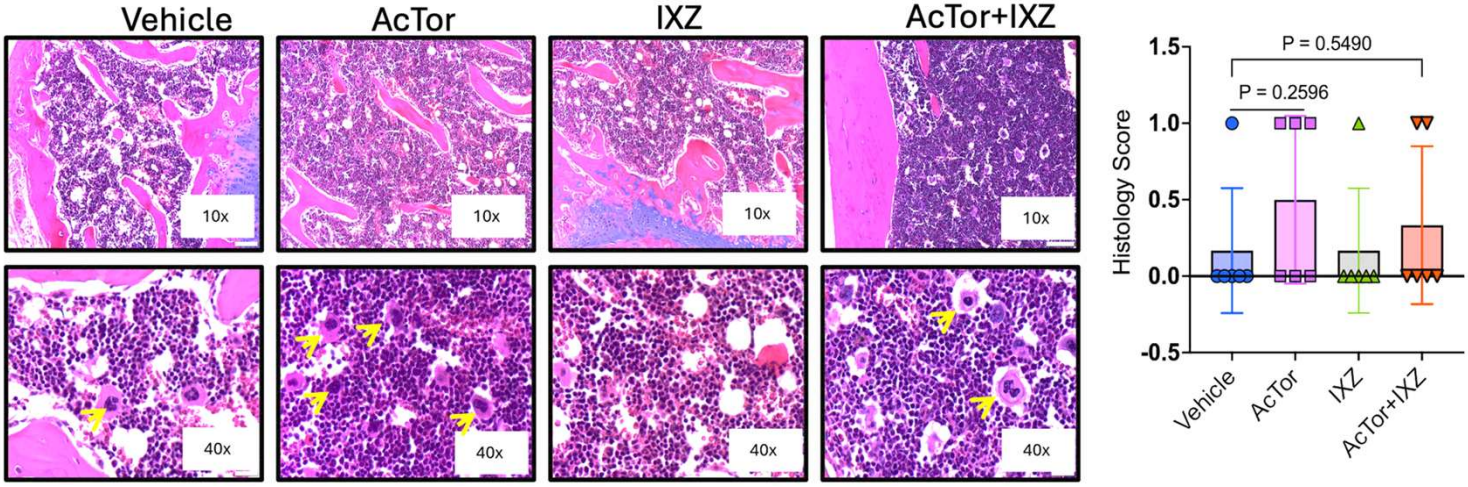

I

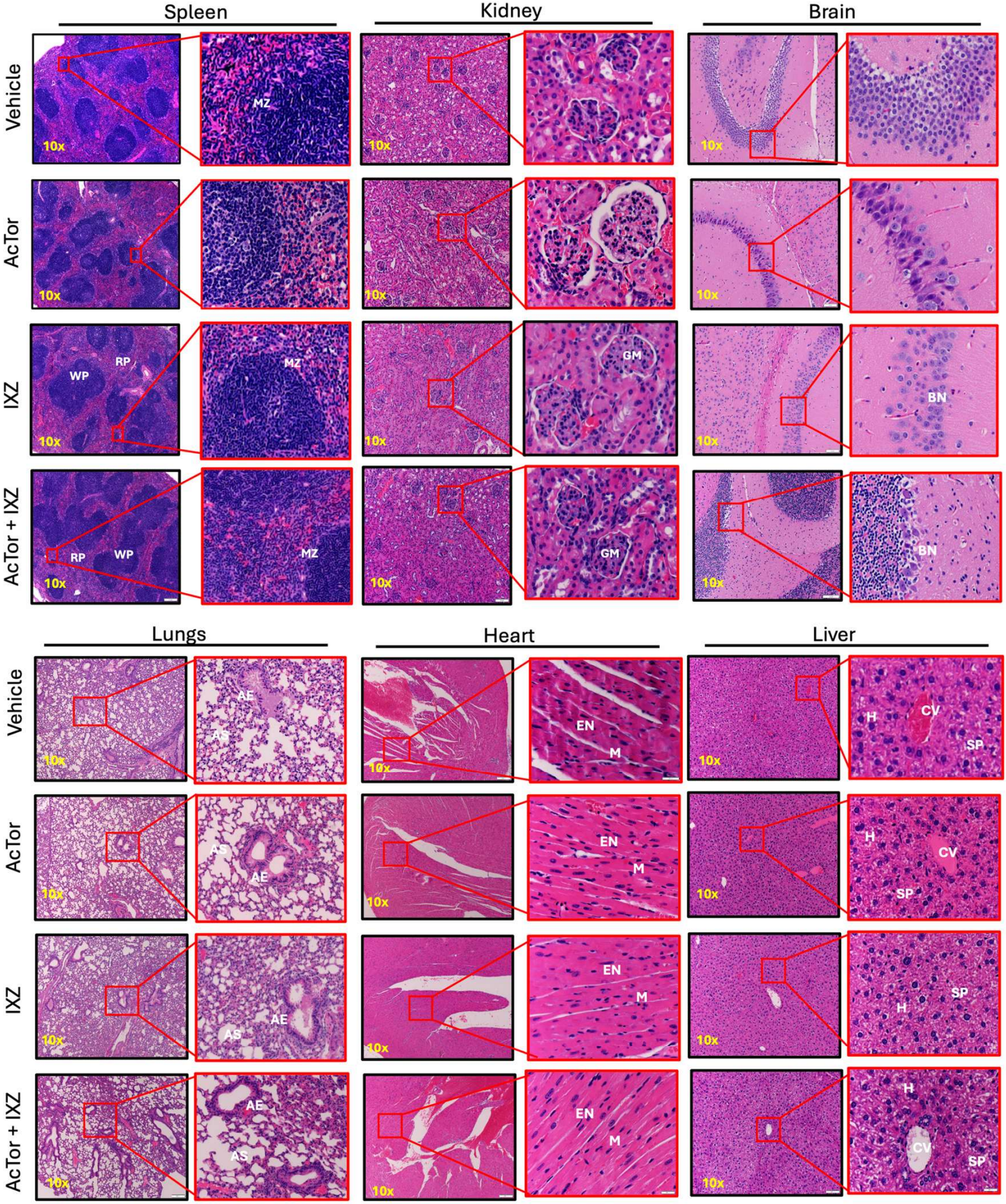

GM : glomeruli
RP : Red Pulp
WP : White pulp

MZ : Marginal zone
BN: basophilic neurons
AE: airways epithelium

AS: alveolar septa
SP : sinusoidal space
CV : Central Vein

H: hepatocytes
EN: nuclei have regular elongate shape
M: myofibrils

Figure S9: AcTor/IXZ treatment does not show evidence of acute toxicity in immunocompetent mice: (A) C57BL/6J mice were treated for three weeks every other day with vehicle, AcTor(30mg/kg), IXZ(1 mg/kg) and AcTor(30mg/kg)+IXZ(1 mg/kg). Mouse weight was recorded biweekly, indicating a gain of weight in all groups, less in IXZ and AcTor/IXZ treated mice. **(B)** Liver transaminases activity in the serum of treated mice. **(C)** Liver histology following a single injection with AcTor at 300 mg/kg. **(D)** Spleen histology of C57BL/6J mice treated a single injection at 300 mg/kg dose did not show any signs of pathology. **(E, F)** Analysis of B cells and T cells percentages in the spleens of the treated mice. **(G)** Total blood counts did not reveal a significant difference between the treatment groups. **(H)** Histology analysis of the bone marrow indicate hypercellularity of megakaryocytes. Score was calculated semi-quantitatively according to Corrao et al (PMID – 36265311). (I) Histology images taken from the different organs of C57Bl/6J treated for three weeks with the indicated drugs show an intact tissue architecture. Data are presented as mean ± SD from n=5 mice. Statistical significance was determined using Brown-Frosythe and Welch one-way ANOVA followed by Dunnett's T3 multiple comparisons test. Calculated *P* values are indicated in the graphs.

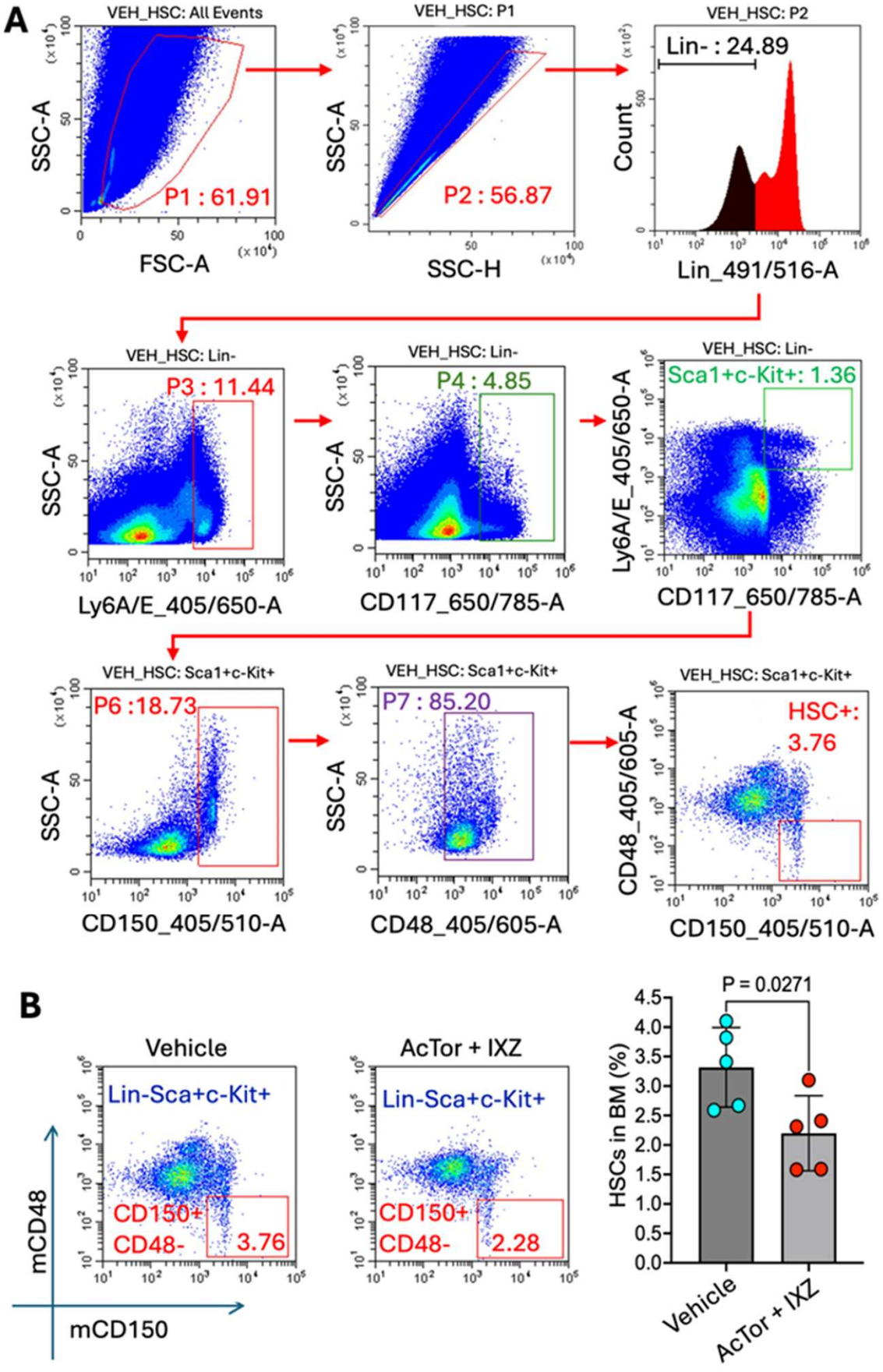

Figure S10: Treatment with AcTor/IXZ for three weeks preserves the HSC compartment in wt mice. (A) C57BL/6J mice were treated for three weeks every other day with IXZ (1 mg/kg) or together with AcTor (30 mg/kg). Shown is the gating strategy for HSCs of the Lin-, Sca1+, cKIT+ cells. HSCs were determined based on CD150+, CD48-. **(B)** Shown is average percentage ± SD of HSCs from total bone marrow population of vehicle and AcTor/IXZ treated mice. Comparison of the two groups was done using a two-tailed unpaired t-test (n=5). Calculated *P* values are indicated in the graphs. Note that the last panel in A is the left panel in B.

A

hCD33+ & hCD45RA+ gating: Spleen of PDX-Mice

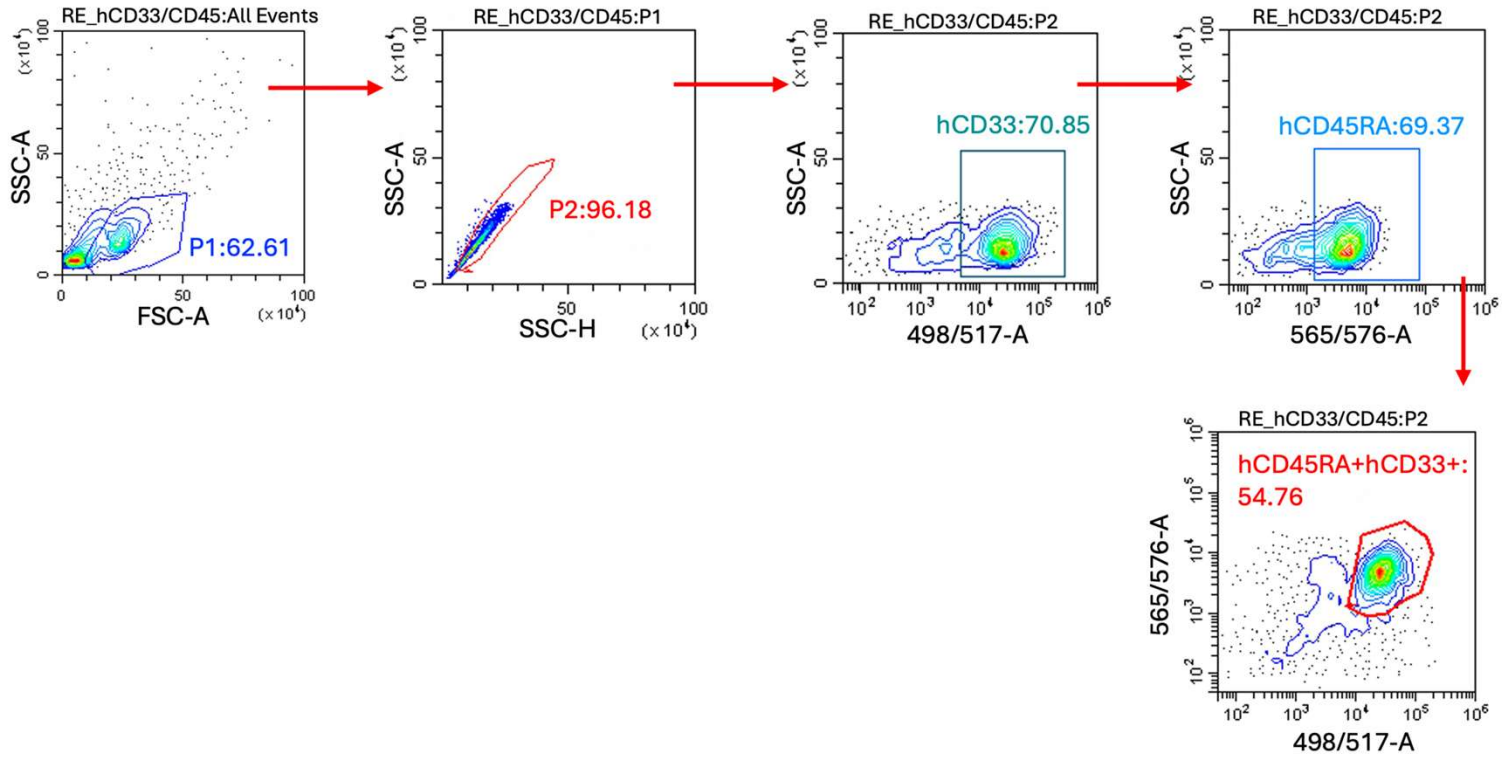

B

hCD33+ / hCD45+ gating with apoptosis : Spleen of PDX-Mice

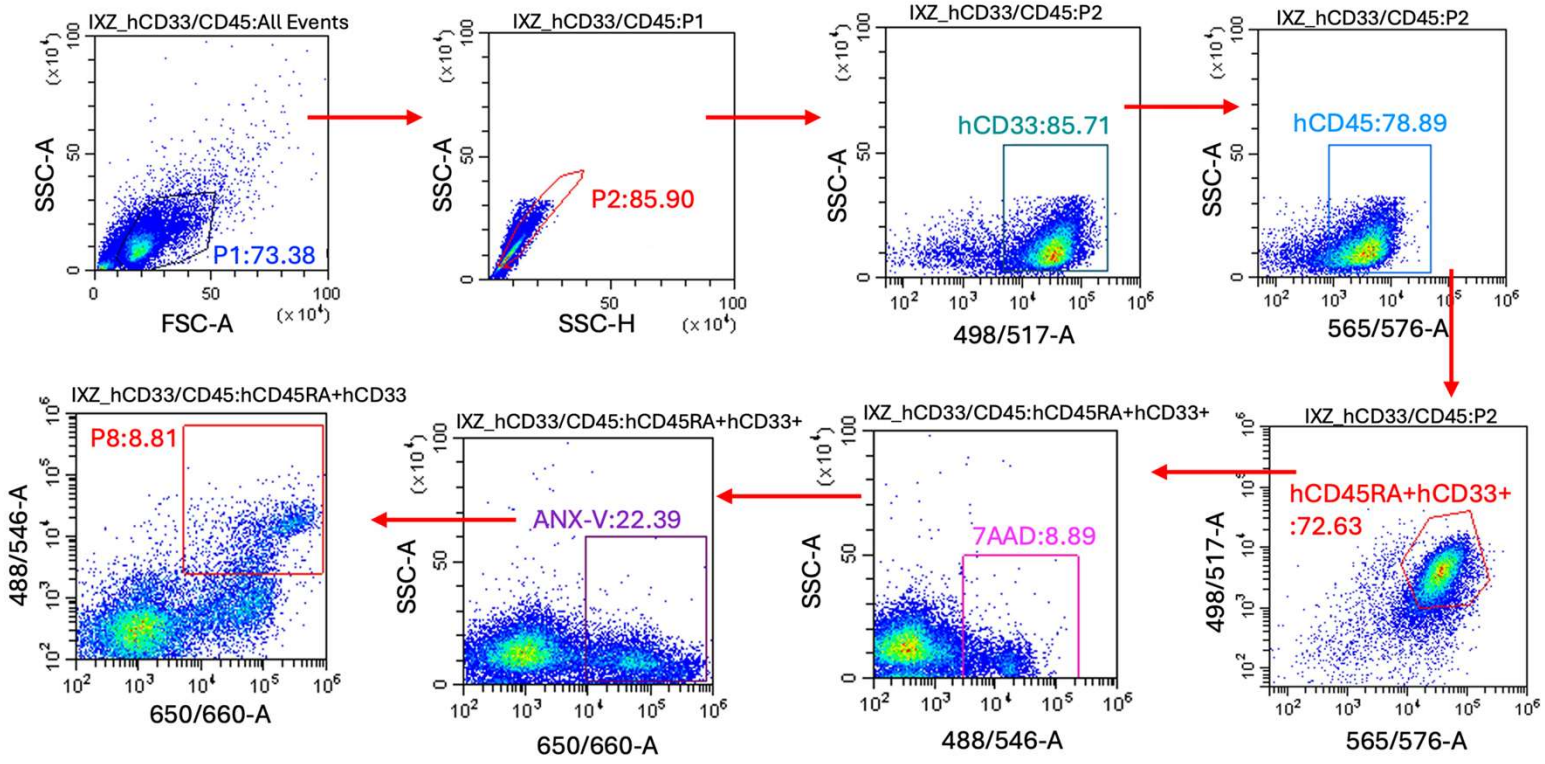

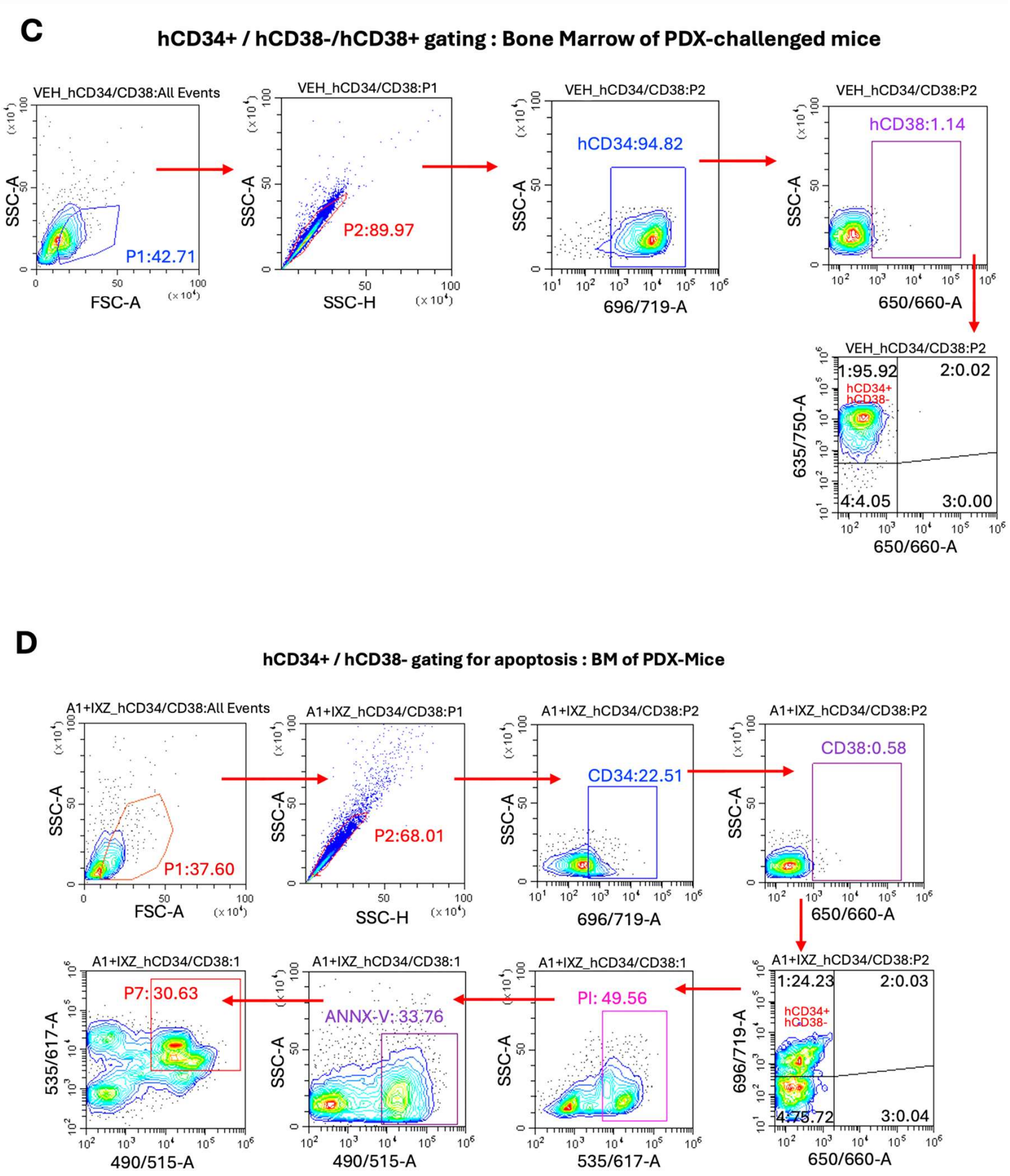

Figure S11: Gating strategies for AML blasts in the spleen and AML stem cells in the bone marrow: (A-D) Shown are the gating strategies for blasts and stem cells, including analysis of apoptosis for both type in PDX-AML model. Note that the final panels are used in the main figures.

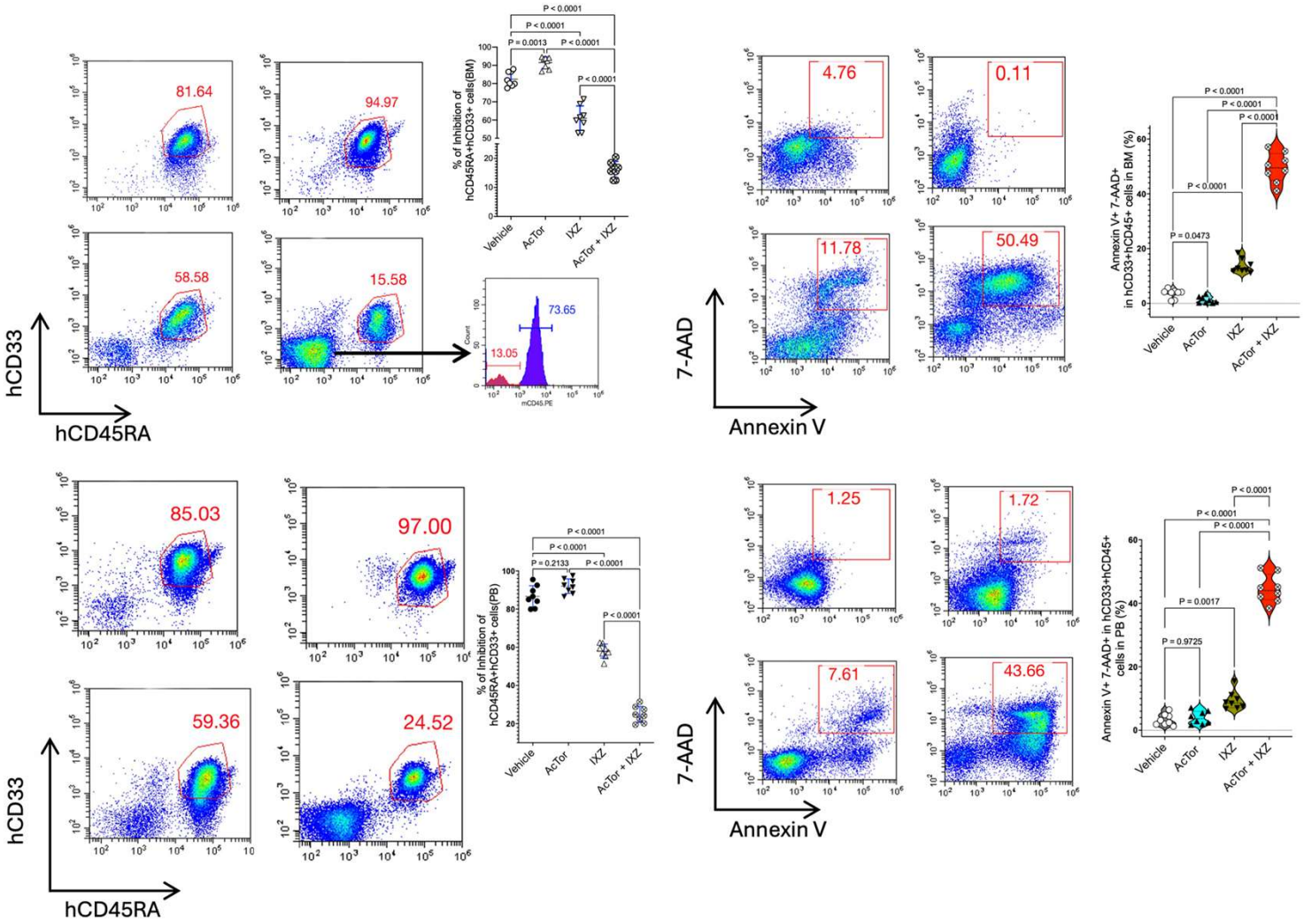

Figure S12: AcTor/IXZ eliminates by apoptosis AML blasts in the bone marrow and blood. Shown are representative results for blast cells in the bone marrow (A) and in the peripheral blood (B) following three weeks of treatment of PDX-induced NSG mice. Data are presented as mean ± SD from n=8 mice. Statistical significance was determined using Brown-Frosythe and Welch one-way ANOVA followed by Dunnett's T3 multiple comparisons test. Calculated *P* values are indicated in the graphs.

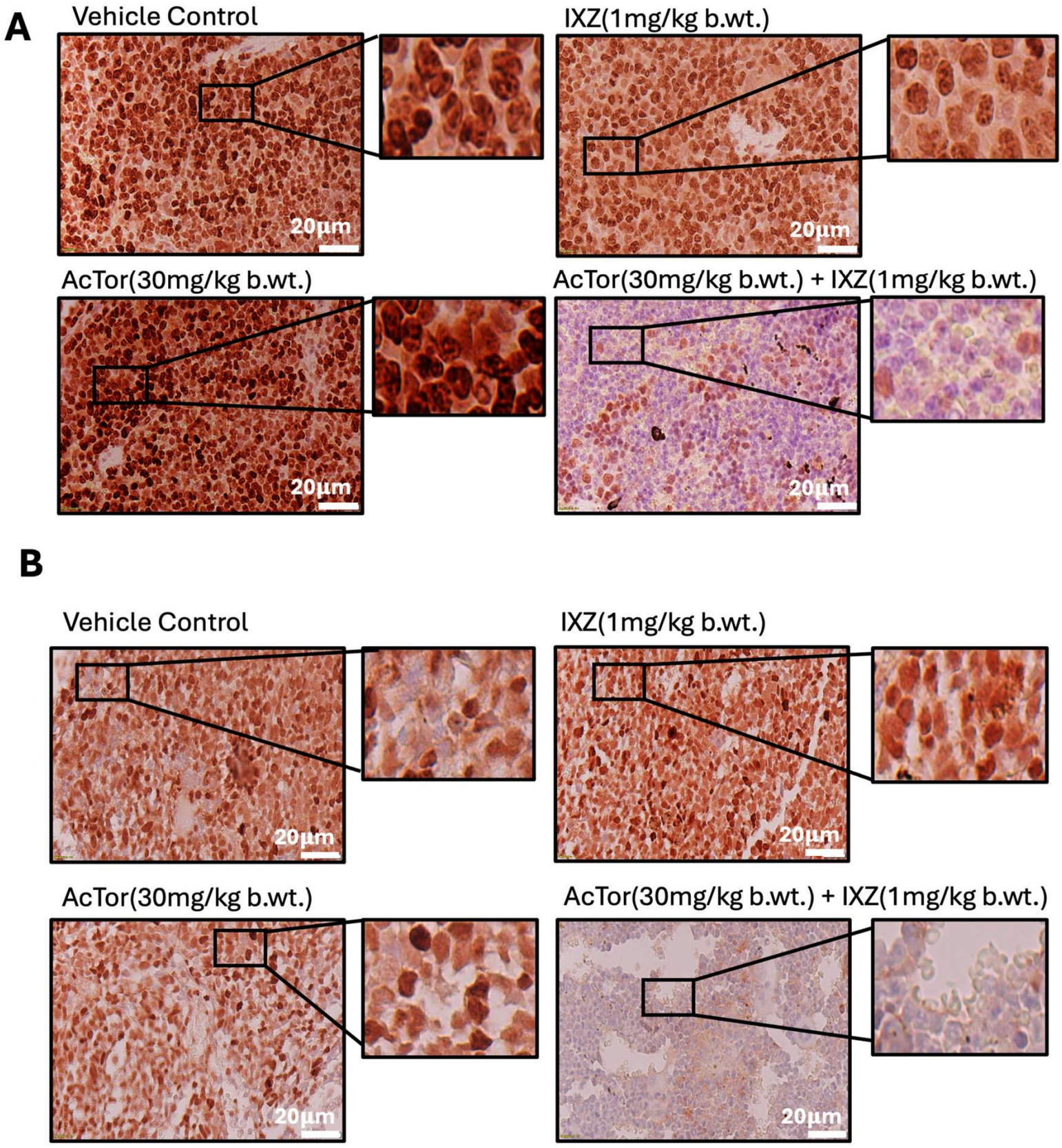

Figure S13: Immunohistochemistry for Ki67 in the (A) spleen and (B) bone marrow of PDX-induced NSG following treatment. Shown is a representative image.

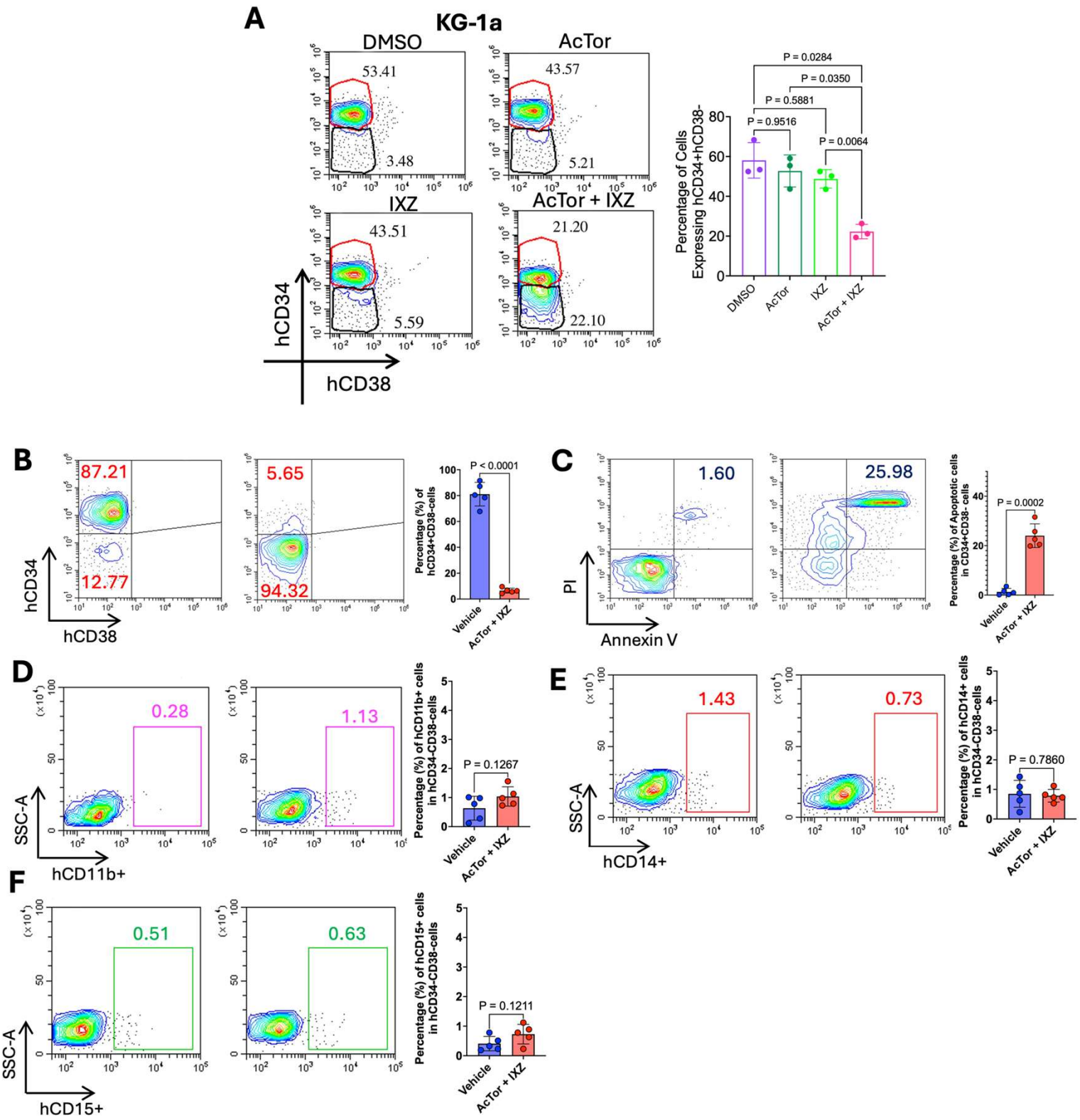

Figure S14: AcTor/IXZ treatment does not induce significant differentiation of AML cells in the BM. KG-1a cells were treated for 24 h and CD34/CD38 expression was analyzed by flow cytometry (n=3). Statistical significance was determined using Brown-Frosythe and Welch one-way ANOVA followed by Dunnett's T3 multiple comparisons test **(B)** Following 3 weeks of AcTor/IXZ treatment expression of CD34 is reduced. The CD34-negative cells were gated and analyzed for apoptosis **(C)**, and differentiation with CD11b **(D)**, CD14 **(E)** and CD15 **(F)**. Data are presented as mean ± SD from n=5 mice. Comparison of the two groups was done using a two-tailed unpaired t-test. Calculated *P* values are indicated in the graphs.

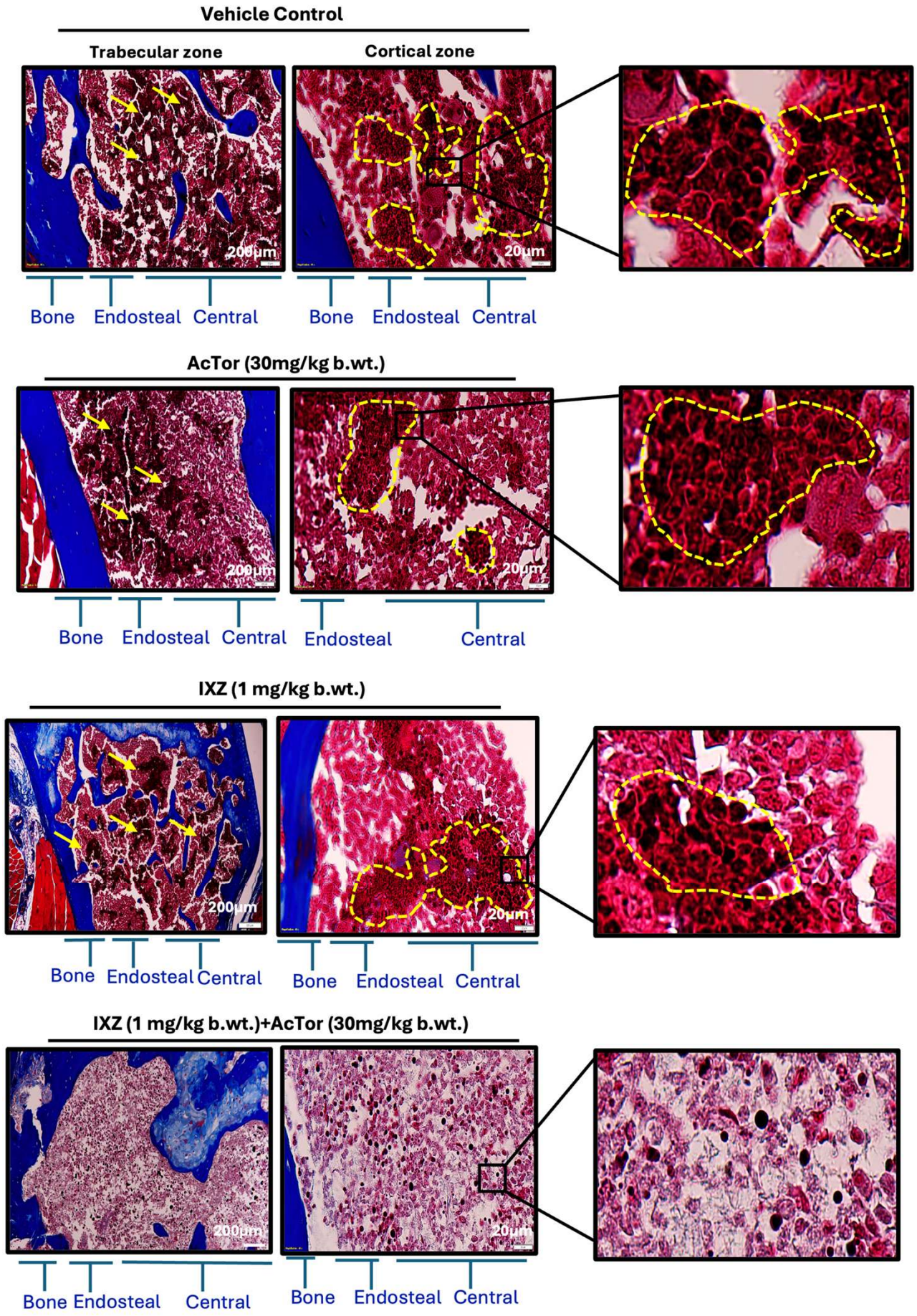

Figure S15: Efficacy of AcTor/IXZ treatment is demonstrated by bone histology. After decalcification, histological sections were stained with Masson's trichrome. Tumor cells' nuclei obtain a dark purple/black color (basophilic nuclei). Arrows mark AML nuclei. Marked are regions of AML engrafted in the bone marrow.

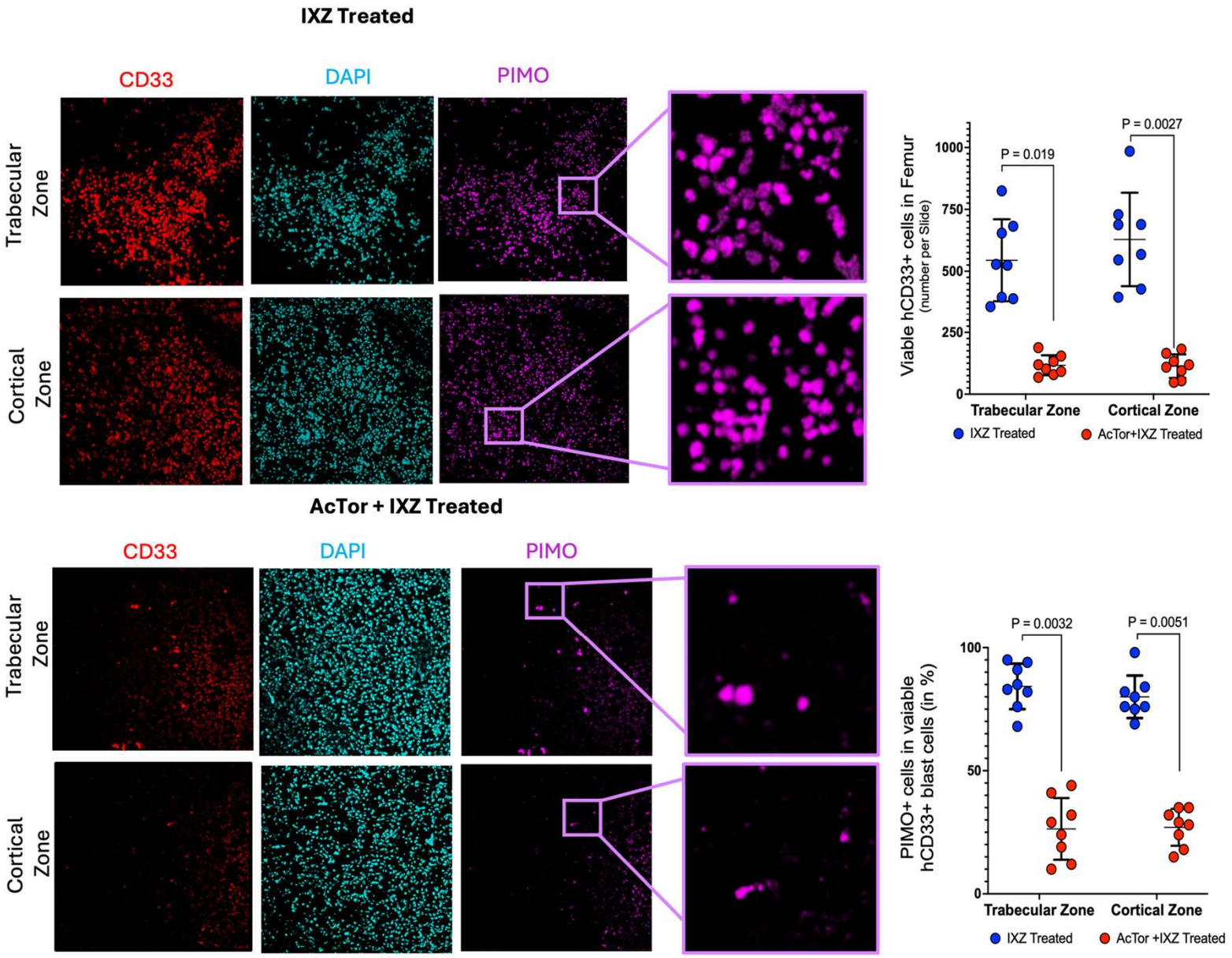

Figure S16: AcTor/IXZ treatment reduces bone marrow hypoxia. NSG mice were challenged with AML PDX cells and five weeks later treated for three weeks with the indicated drugs. Pimonidazole (PIMO) was injected prior to sacrifice. Femur bones were isolated, decalcified, and histological sections were stained for PIMO and anti-CD33 to show the proximity between tumor cells and local hypoxia. Eight slides were quantified independently from each group. Data are presented as mean ± SD from n=8 mice. Comparison of the two groups was done using a two-tailed unpaired t-test. Calculated *P* values are indicated in the graphs.

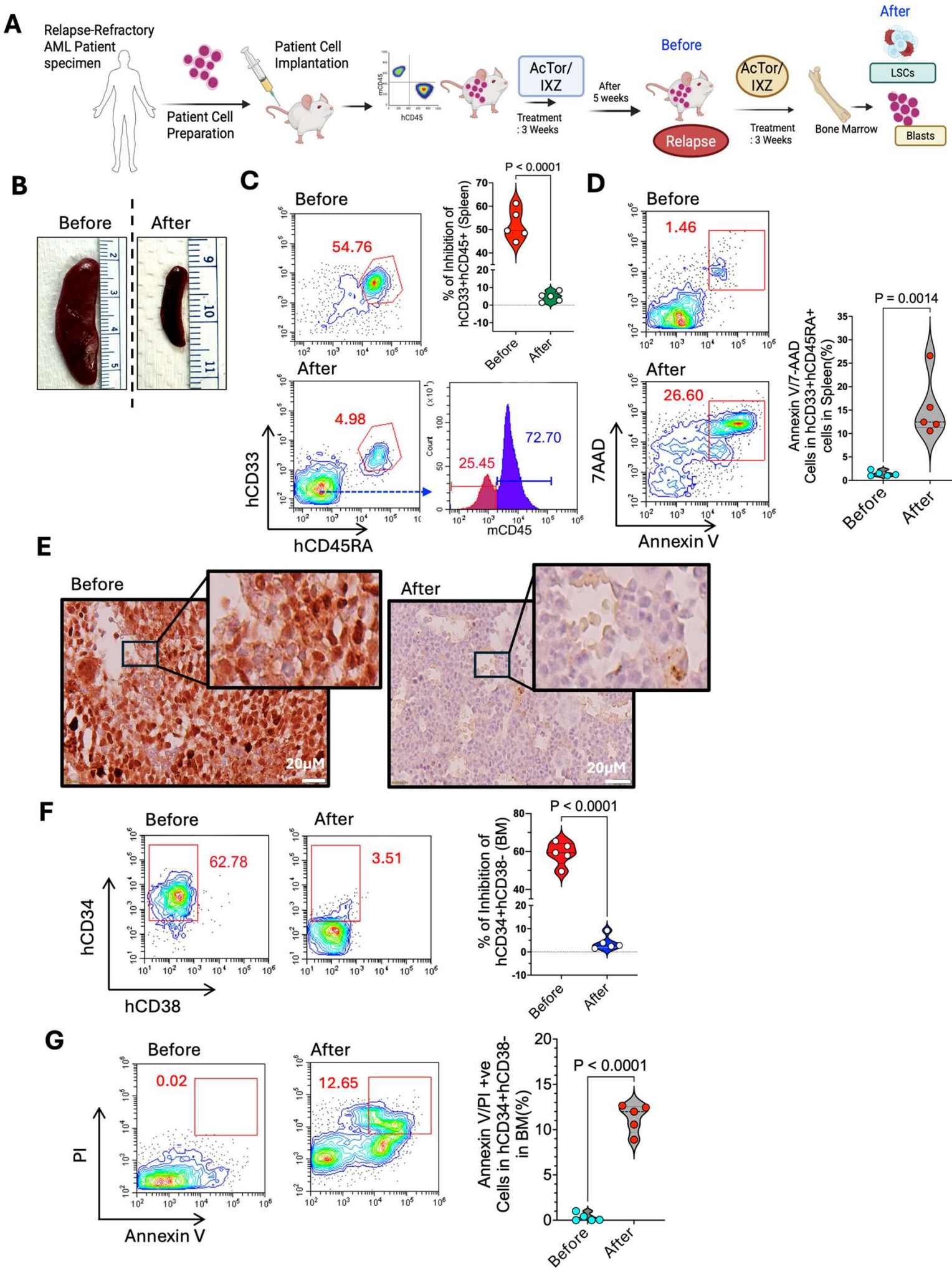
A
Relapse-Refractory AML Patient specimen
Patient Cell Preparation
Patient Cell Implantation
hCD45
mCD45
AcTor/ IXZ
Treatment : 3 Weeks
After 5 weeks
Before
Relapse
AcTor/ IXZ
Treatment : 3 Weeks
Bone Marrow
After
LSCs
Blasts
B
Before
After
C
Before
54.76
After
4.98
hCD33
hCD45RA
25.45
72.70
Count
mCD45
P < 0.0001
% of Inhibition of hCD33+hCD45+ (Spleen)
Before
After
D
Before
1.46
After
26.60
7AAD
Annexin V
P = 0.0014
Annexin V/7-AAD Cells in hCD33+hCD45RA+ cells in Spleen(%)
Before
After
E
Before
After
20μM
20μM
F
Before
62.78
After
3.51
hCD34
hCD38
P < 0.0001
% of Inhibition of hCD34+hCD38- (BM)
Before
After
G
Before
0.02
After
12.65
PI
Annexin V
P < 0.0001
Annexin V/PI +ve Cells in hCD34+hCD38- in BM(%)
Before
After

Figure S17: Treatment with AcTor/IXZ maintains potency following AML relapse. (A) NSG mice were engrafted with patient-derived AML cells. When more blood contained more than 75% of human CD45+ cells, treatment was initiated every other day for three weeks with AcTor/IXZ. Mice were left to recover for five weeks and then divided into two cohorts: untreated (termed “Before”) or treated again with AcTor/IXZ (termed “After”). **(B)** Shown is a representative spleen form each of the groups. **(C)** Flow cytometry analyses of spleen cells for AML blasts and quantification. Note that mouse hematopoietic cells populate the spleen for the second time. **(D)** Analysis of the CD45+/CD33+ AML cells for apoptosis using 7-AAD/Annexin V staining. **(E)** Typical immunohistochemistry images of bone marrow for Ki67 from before and after a second treatment with AcTor/IXZ. **(F)** Flow cytometry analyses of bone marrow for AML stem cells and quantification. Bone marrow AML cells reduced expression of the stem cell marker CD34 following a second treatment with AcTor/IXZ. **(G)** Analysis of CD34+ AML cells for apoptosis using PI/Annexin V staining. Data are presented as mean ± SD from n=5 mice. Comparison of the two groups was done using a two-tailed unpaired t-test. Calculated *P* values are indicated in the graphs.

Videos demonstrating the drug's efficacy in TP53^PDX bearing mice

Figure S18: Representative images of TP53^PDX-bearing mice. (A) Vehicle-treated control group, (B) mice treated with IXZ (1 mg/kg body weight), and (C) mice treated with the combination of AcTor (30 mg/kg body weight) and IXZ (1 mg/kg body weight). After three weeks of treatment, mice in the combination group (C) appeared more active and exhibited improved mobility compared to those in the vehicle or IXZ-alone groups.

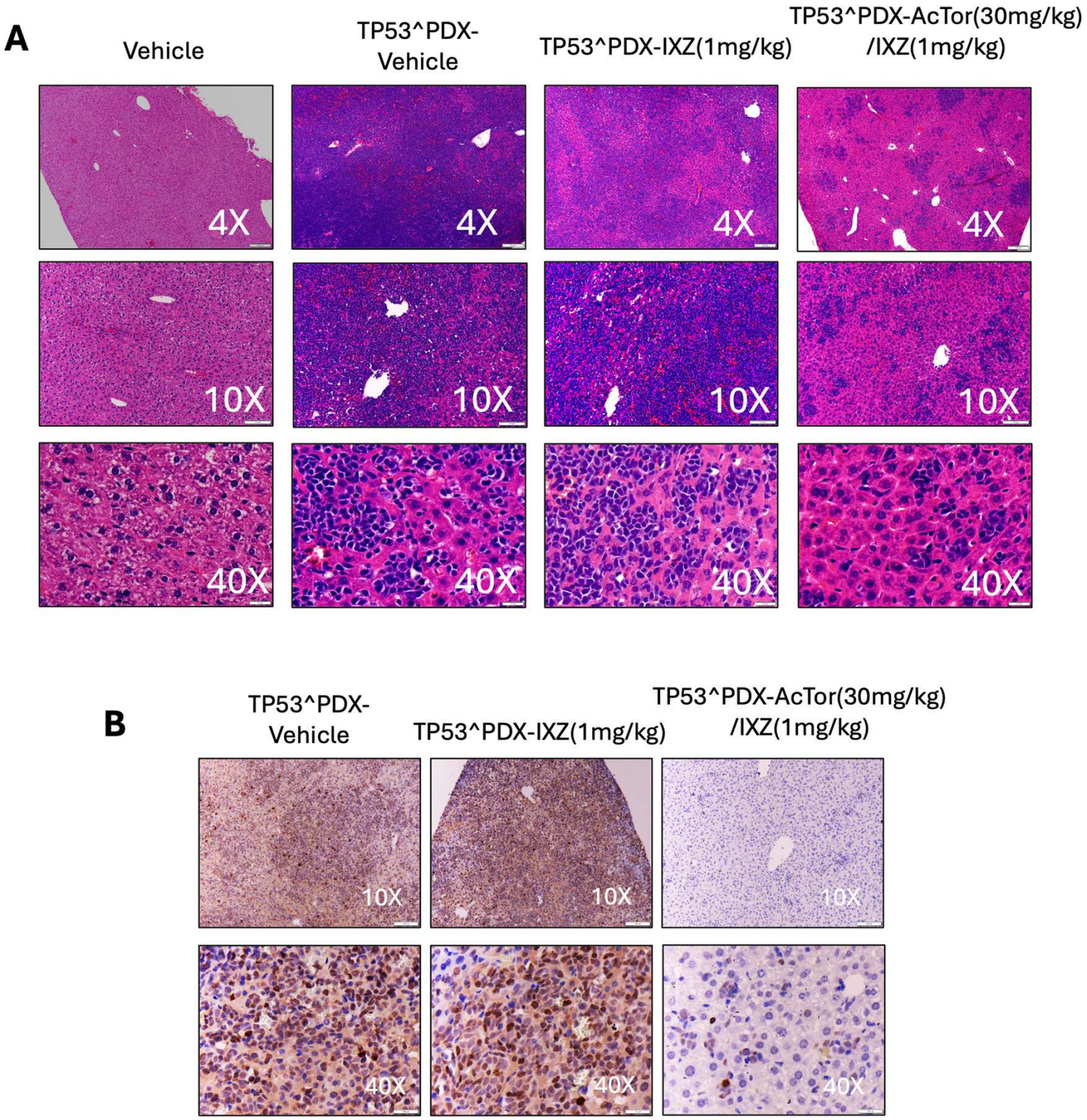

Figure S19: Combination treatment with AcTor (30 mg/kg) and IXZ (1 mg/kg) reduced hepatic infiltration of TP53^PDX tumor cells in treated mice. (A) Hematoxylin and eosin (H&E) staining of liver sections shows metastatic tumor cell infiltration, which was markedly decreased in the combination treatment group compared to vehicle- or IXZ-alone–treated animals. (B) Ki67 immunostaining further confirms a reduction in proliferating ($Ki67^{+}$) cells within the liver of mice receiving the combination therapy.